V European Conference on Computational Fluid Dynamics
ECCOMAS CFD 2010
J. C. F. Pereira and A. Sequeira (Eds.)
Lisbon, Portugal, 14-17 June 2010

IMMERSED BOUNDARY METHOD PREDICTIONS OF SHEAR STRESSES FOR DIFFERENT FLOW TOPOLOGIES OCCURRING IN CEREBRAL ANEURYSMS

Julia Mikhal[*], David J. Lopez Penha[*], Cornelis H. Slump[†] and Bernard J. Geurts[*,‡]

[*] Multiscale Modeling & Simulation, Dept. of Applied Mathematics, University of Twente, P.O. Box 217, 7500 AE Enschede, The Netherlands.
e-mail: {julia.mikhal, d.j.lopezpenha, c.h.slump, b.j.geurts}@utwente.nl
[†] Signals and Systems, Dept. of Electrical Engineering, University of Twente, P.O. Box 217, 7500 AE Enschede, The Netherlands.
[‡] Anisotropic Turbulence, Dept. of Applied Physics, Eindhoven University of Technology, P.O. Box 513, 5600 MB Eindhoven, The Netherlands.

Key words: Immersed boundary method, volume-penalization, incompressible flow, shear stress, cerebral aneurysm

Abstract. *A volume-penalizing immersed boundary method is presented that facilitates the computation of incompressible fluid flow in complex flow domains. We apply this method to simulate the flow in cerebral aneurysms, and focus on the accuracy with which the flow field and the corresponding shear stress field are computed. The method is applied to laminar, incompressible flow in curved cylindrical vessels and in a model aneurysm. The time-dependent shear stress distributions over the vessel walls are visualized and interpreted in terms of the flow fields that develop. We compute shear stress levels at two different Reynolds numbers, corresponding to a steady and an unsteady flow. In the latter situation strong fluctuations in the shear stress are observed, that may be connected to raised risk-levels of aneurysm rupture.*

1 INTRODUCTION

The prediction of flow that arises inside complex cavities and vessels is a key application area for immersed boundary (IB) methods [1]. We consider the development and application of a volume-penalizing IB method for the computation of flow inside cerebral aneurysms [2]. Monitoring and predicting possible rupture of such aneurysms constitutes a timely challenge in view of the growing medical attention to these health risks [3]. To understand such risks one needs to develop the capability to predict the detailed flow behavior and corresponding shear stresses and to translate these into risk-categories. Such capability allows a more complete planning of surgical intervention and can be used to predict the effectiveness of such procedures. In this paper we discuss the basic IB method and illustrate its capability to predict shear stresses in model aneurysms, provided adequate spatial resolution of the flow field.

We employ a volume-penalization IB method in which the flow domain is characterized by a so-called 'masking function'. In particular, we introduce a binary function such that solid and fluid parts in the domain are identified by a value of '1' and '0', respectively. This method of representing a complex shaped domain allows for a range of sources for specifying the geometry. In medical applications the shape of cerebral aneurysms developing in patients can be inferred from three-dimensional rotational angiography [4]. This procedure yields a large number of slices through a small section of brain tissue, allowing an approximate identification of the fluid and the solid parts, and hence specify the masking function. The raw angiography data allows for a simple 'staircase approximation' of the vessel and aneurysm shape in which individual pixels in the digital data form the smallest unit of localization of the solid-fluid interface. We will adopt the 'staircase' geometry representation in this paper and do not yet incorporate smoothed geometry reconstruction methods.

Common locations for the formation of cerebral aneurysms are at 'T' and 'Y'-shaped junctions in vessels of the 'Circle of Willis' [5]. This is a central vessel network for the supply of blood to the human brain. To understand the key 'T' and 'Y' risk-areas in the Circle of Willis, the flow in basic vessel and aneurysm structures should be analyzed. Such a 'library' of elemental shapes includes straight and smoothly curved cylindrical vessels, and spherical cavities. We simulate the Navier-Stokes equations for incompressible flow on Cartesian grids, using the IB method in order to understand the fluid mechanical properties of these 'elemental' structures.

The accuracy with which the flow field in a complex geometry can be computed on the basis of an IB method depends strongly on the spatial resolution of the smallest details of the domain. In case of cerebral aneurysms, the domain is not specified beyond a modest spatial resolution. Hence, it is important to consider the issue of how sensitive predictions depend on the quality of the geometrical characterization. For medical applications, it is particularly relevant to find out which 'robust' conclusions can be drawn from simulations, and what aspects remain unclear because of uncertainties in the actual flow conditions

and the geometry. This issue can be addressed in detail using computational modeling.

The convergence of IB-predictions toward the actual solution of the Navier-Stokes equations is a key element that decides about the usefulness of this approach for realistic applications. We analyze this in detail for Poiseuille flow in a cylindrical tube. The non-alignment of the geometry with the Cartesian grid is shown to imply only first order convergence in case of flow in a cylindrical tube. The precise definition of the masking function in the near-wall region has a strong influence on the error-levels that are obtained. A definition in which the numerical flow domain is entirely inside the physical flow domain of the problem considered is found to be beneficial for reducing the error levels.

The flexibility of the IB method is illustrated with a study of the flow in a model cerebral aneurysm. We adopt an energy-conserving finite-volume discretization that is, by construction, stable on any spatial resolution [6]. In these applications only the masking function needs to be specified properly and the spatial resolution should be fine enough to capture, at least qualitatively, the smallest geometrical details. From the study of Poiseuille flow we infer that about 16 grid points per 'opening' in the flow-domain suffices to obtain reliable predictions. This brings a large range of laminar and transitional flows in realistically complex geometries within reach of large-scale computing. In this way, numerical flow simulation in combination with the IB approach can provide reliable information about the flow structure and associated stress levels, that would otherwise not be attainable from clinical inference. Such computational modeling augments current clinical data and can, in future, help improve the planning and execution of surgical interventions; allowing different scenarios to be tested before actual surgery is undertaken.

The organization of this paper is as follows. In Section 2 we present a brief sketch of the IB method that is adopted and discuss the convergence of numerical predictions to the exact analytical solution in case of Poiseuille flow. The application of the IB method to flow in cerebral aneurysms is discussed in Section 3 and an analysis of shear stress levels is given in Section 4. Concluding remarks are in Section 5.

2 Immersed boundary method for incompressible flow

In this section we give a brief review of the volume-penalization immersed boundary (IB) method that is considered in this paper and analyse the Poiseuille flow in a tube. We focus on incompressible fluids whose dynamics is governed by the conservation of mass and momentum:

$$\partial_j u_j = 0 \tag{1}$$

$$\partial_t u_i + \partial_j (u_j u_i) + \partial_i p - \frac{1}{Re} \partial_{jj} u_i - f_i = 0 \tag{2}$$

where ∂_t and ∂_j denote partial derivatives with respect to time t and spatial coordinate x_j, u_j denotes the velocity component in the x_j direction and p is the pressure. The Reynolds number $Re = UL/\nu$ is a measure for the relative importance of the nonlinear convective fluxes and the linear viscous fluxes [7]; it is expressed in terms of a reference

velocity scale U, a reference length-scale L and the kinematic viscosity $\nu = \mu/\rho$ with molecular viscosity given by μ and the fluid mass-density ρ. The forcing f_i can be used to represent a variety of physical mechanisms that influence the evolution of the flow. Here, we will use this forcing for another purpose, i.e., to approximate no-slip conditions at solid boundaries that are contained in the domain [1].

The IB method enjoys a growing interest in the field of computational science. It provides a strong alternative to conventional numerical simulation methods in case flow in and around very complex spatial shapes is considered. Conventional methods adhere to computational meshes that are body-fitted. With this approach the gridding of the fluid region becomes very time consuming for complex domains. The task of generating grids that yield an accurate discrete computational model is correspondingly difficult, up to the point of becoming impractical. Instead, the IB method can be formulated entirely in terms of a uniform Cartesian grid. The geometry over and through which the flow takes place is simply immersed in a 'block' of physical space. These striking differences in the computational strategies also imply important consequences for the accuracy with which flow near solid boundaries may generally be captured. Conventional body-fitted methods allow, in principle, for a precise representation of no-slip conditions at the body. In contrast, the accuracy achieved by an IB method generally suffers from the non-alignment of the interface between solid and fluid regions with the Cartesian grid. This is even more challenging if, next to the flow velocity, information about the gradient of the velocity is desired. For such situations we identify spatial resolution requirements that are needed to yield reliable results.

We employ a basic IB method in which the forcing term f_i represents a volume penalization. The impenetrability of a stationary solid wall to fluid flow is approximated by direct penalization of the flow from entering the solid domain. This is represented here by a forcing term

$$f_i = -\frac{1}{\varepsilon}\Gamma(\mathbf{x})u_i(\mathbf{x},t) \tag{3}$$

in which the control parameter $\varepsilon \ll 1$ (a typical value used is $\varepsilon = 10^{-10}$) and $\Gamma(\mathbf{x})$ denotes the so-called 'masking function' or 'phase indicator' which assumes the value '1' in case the point $\mathbf{x}$ belongs to a solid part of the domain and '0' is case it is located in an open fluid-filled part of the domain. In this way the entire domain Ω is decomposed into a solid part Ω_s and a fluid part Ω_f; while in Ω_f the forcing is absent and the original, incompressible Navier-Stokes equations govern the flow, the various fluxes in the momentum equation are entirely overruled by the IB forcing inside Ω_s.

The form of the forcing f_i inside the solid part implies that the velocity components u_i are negligible; if at some location in the solid u_i would, for some reason, have become non-zero then the forcing drives the local velocity very fast back to negligible values. In the region near the interface between the solid and the fluid parts of the domain the velocity field would be forced to negligible values within a very thin strip of the grid. A sufficiently small value of ε will imply a very localized region in which a non-trivial flow

in Ω_f connects to a solution with negligible values in Ω_s. This rough sketch identifies that the simple volume forcing (3) can indeed approximate a no-slip boundary condition, localized to within one grid-cell.

The equations resulting from the introduction of the forcing (3) in the Navier-Stokes equations need to be treated numerically. We adopt a finite-volume discretization that preserves the skew-symmetry of the nonlinear convective fluxes and the positive-definite dissipative nature of the viscous fluxes [6]. In particular, this method can be shown to be stable on any (coarse) resolution, without having to resort to artificial dissipation that would smear out small-scale details in a numerical solution. This is particularly significant in case turbulent flow is simulated with dynamically important fluid motions on a wide spectrum of scales. Also for laminar flows in a complex domain the use of such a discretization is important. In order to capture forces on the solid walls of the domain the treatment of the small near-wall flow structures is essential. A second order accurate method for the fluxes is employed, implemented on a staggered grid. The effect of these fluxes is integrated in time using an explicit time-stepping algorithm of Adams-Bashforth type [6, 8]. The contribution of the forcing term $\mathbf{f}$ is integrated implicitly in time, which overcomes severe stability problems that would arise with explicit methods as $\varepsilon \ll 1$.

The staggered grid arrangement poses the particular question how exactly the masking function Γ should be defined. Globally, Γ is easily defined as indicated above. However, there is some freedom in its definition on grid-scale near a solid-fluid interface. In this paper, first, we choose to work with an individual grid cell as the smallest elementary unit; this implies that a grid cell is considered either as part of the solid or as part of the fluid. If the center of the cell is solid or fluid, then we assign this property for the entire grid cell. Second, we need to identify which component of the solution is used as basis for the masking function. In fact, as all three velocity components u_i and the pressure p are defined on their respective grids, one may consider Γ_{u_i} or Γ_p. Also, combinations of these are possible in principle, e.g., the sum of all velocity-based masking functions. We choose to work with Γ_p, which defines the precise location (within the resolution of the adopted grid) of the solid-fluid interface in a 'staircase' approximation.

The convergence of the volume-penalization IB method is studied on the basis of laminar Poiseuille flow in a straight cylindrical tube. This test-case allows comparison with the exact analytical solution as point of reference. The cylindrical tube application tests the IB method for geometries that are not aligned with the Cartesian grid. Poiseuille flow is one of the few exact solutions to the incompressible Navier-Stokes equations [7]. In case of flow through a cylinder aligned with the x_1 axis, the Poiseuille profile is given by

$$u_1(r) = U_{max}(1 - r^2) \tag{4}$$

where $0 \leq r \leq 1$ is the radial coordinate and U_{max} the maximal velocity in the center of the tube. This parabolic profile provides a strict test for the IB method; in the sequel we investigate the achieved accuracy as a function of spatial resolution.

The accuracy for the IB method is studied for three, slightly different, methods of

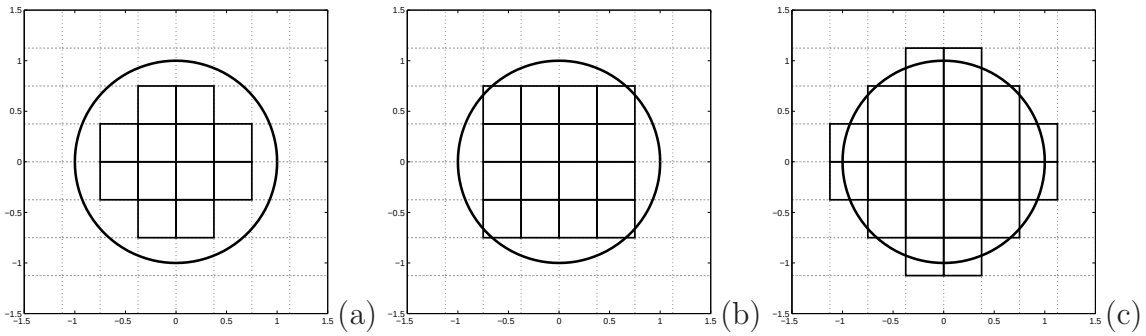

Figure 1: Definition of the 'inner' (a), 'middle' (b) and 'outer' (c) strategy for defining the masking function across a cylindrical tube. Either all four grid points are in the fluid (a), or at least three (b) or at least two (c) to distinguish the different strategies. Grid cells that are identified with the fluid region are drawn in thicker lines.

identifying the masking function. These are sketched in Fig. 1; we refer to these as 'inner', 'middle' and 'outer', depending on the criterion when exactly a grid cell is counted as part of the *fluid* region. In the 'inner' strategy a grid cell is considered part of the fluid if all four of its corner-points are in the fluid region. The 'middle' strategy also includes grid cells that share 3 of its corner points with a fluid region and the 'outer' strategy further allows grid cells with only 2 corner points in the fluid. We performed simulations on a range of grids for this flow problem and investigated the accuracy of predictions for the inner-middle-outer strategies.

The convergence of the numerical results, as measured in the discrete L_2-norm is collected in Fig. 2. We observe that all three strategies display first-order convergence. This appears consistent with the results obtained for the plane channel flow in case the no-slip condition is imposed within a grid cell of the solid wall [9]. In case of a cylindrical tube, the non-alignment of the Cartesian grid with the precise geometry implies that the approximate no-slip condition in the IB method is in all points within half a grid cell. We observe a strong dependence of the level of the error on the masking strategy, with a strong improvement in the L_2-norm if we use a masking function for the fluid region that is entirely inside the flow domain, i.e., 'retracted' by about half a grid cell from the actual location of the cylinder wall. This relation between the error-level and the precise definition of the masking function near solid walls was also observed in case of Poiseuille flow in a planar channel [9]. We will exploit this property in the future to achieve higher accuracy in more general geometries – this is a topic of ongoing investigations.

3 IB predicted flow topologies in model aneurysms

In this section we illustrate the application of an immersed boundary method to flow in curved vessels and model aneurysms. The flow domain is composed of a simple sinusoidally shaped cylindrical tube of radius R to which we add a spherical cavity of radius $3R$, thus

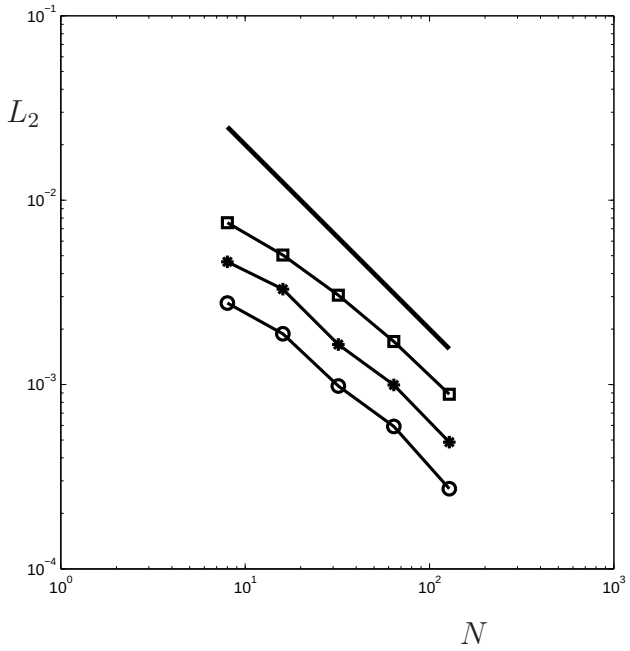

Figure 2: Convergence of the discrete L_2-norm of the error in the numerical solution compared to the exact Poiseuille profile, as a function of the spatial resolution N. The solid curve denotes first order convergence and the labels are such that 'squares' denote the 'outer', 'asterisks' the 'middle' and 'circles' the 'inner' strategy for the definition of the masking function.

arriving at a configuration that generates significant flow separation. This has a strong influence on the stability of the flow and on the forces that develop on the vessel walls.

In Fig. 3 we display an impression of the developing flow in the model geometries. The flow is simulated at a Reynolds number $Re = 100$, based on the tube diameter, the mass flow rate and the kinematic viscosity of water. An unsteady solution develops, of which a snapshot is shown. The effect of the IB masking function for the solid region is clearly observed in terms of the regions of 'essentially' zero velocity outside the flow domain. The connection with the flow inside the tube appears to be correctly captured – the approximate no-slip condition is expressed in a very narrow strip of the Cartesian grid, as is desired from the volume-penalization method. The addition of a spherical cavity is seen to affect the flow in the curved tube, which leads to the development of a detached 'jet' that proceeds to flow toward the wall of the cavity, producing a vortical structure that fills a large part of the spherical cavity with recirculating flow. The occurrence of such flow structures contributes to an extension of the average 'residence time' of blood inside the flow domain, expressing a deterioration of the quality of transport of nutrients to, and waste products from the tissue surrounding the aneurysm. This can be an important indicator for the rate at which health risks may develop.

The main challenge for the IB method in case of flow through model aneurysms is in capturing the flow near the solid-fluid interface, which is required to compute the shear

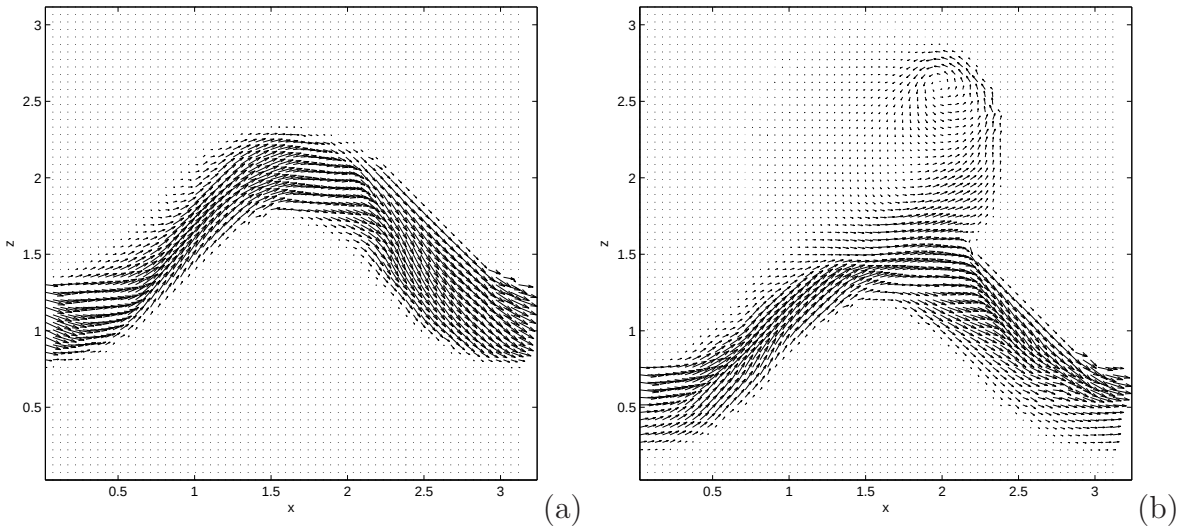

Figure 3: Snapshot of the developing flow inside a curved cylindrical tube at $Re = 100$, without (a) and with (b) a spherical cavity attached. The flow is visualized in a cross-section through the geometry, by plotting the in-plane velocity vectors.

stress. We define the shear stress in terms of the gradient of the velocity as follows. The rate of strain tensor $\boldsymbol{S}$ is such that

$$S_{ij} = \frac{1}{2}\Big(\partial_i u_j + \partial_j u_i\Big) \tag{5}$$

The shear stress ξ is a measure for the off-diagonal components of $\boldsymbol{S}$. We introduce $\Xi_{ij} = S_{ij}$ if $i \neq j$ and $\Xi_{ii} = 0$. Then,

$$\xi^2 = \Xi_{ij}\Xi_{ij} \tag{6}$$

The distribution of the shear stress ξ across the vessel wall is an important indicator for the forces that act on the wall. This makes the shear stress a key quantity of relevance for the prediction of long-term risk of rupture of the aneurysm wall.

In Figs. 4 and 5 the normalized shear-stress distributions are shown at a characteristic stage in the development of the flow. We observe that the detached jet that was discussed above, impinges on the wall of the spherical model aneurysm and creates a region of intensified shear stress at $Re = 100$. The shear stress ξ is also quite large near 'extremities' of the curved cylindrical tube that is connected to the sphere. Cross-sections of the model aneurysm (Fig. 5) show the distribution of the shear stress which is maximal close to the vessel walls. From these plots the differences in flow structures at $Re = 10$ (Fig. 5(a)) and at $Re = 100$ (Fig. 5(b)) can be directly observed. In particular, we observe that the flow hardly penetrates the spherical cavity in case $Re = 10$ while a significant separated vortex is seen to dominate the stress distribution on the cavity wall at $Re = 100$. The IB

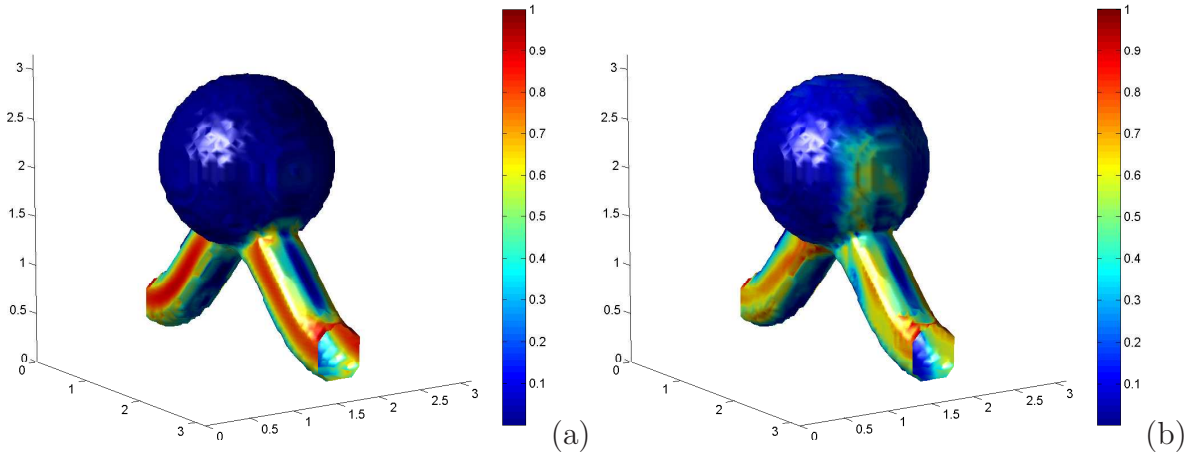

Figure 4: Predicted 'normalized' shear-stress distribution over the vessel wall of a model aneurysm, composed of a curved cylindrical tube onto which a spherical cavity is attached. The stress levels are normalized with respect to the maximal value in the domain. The steady flow at $Re = 10$ (a) and the unsteady flow at $Re = 100$ (b) are obtained and a characteristic impression of the shear stress is shown. The spatial resolution that was adopted is $64 \times 64 \times 64$.

method appears to provide a reliable impression of the distribution of the shear stress, showing the flexibility of the approach. A detailed analysis of the accuracy with which ξ is predicted requires a full grid-refinement study, which is the subject of an upcoming publication.

4 Shear stress distribution in model aneurysms

In this section we analyze the shear stress that develops inside curved vessels and in our model aneurysm. We concentrate on the maximum shear stress that arises over all the vessel walls, i.e.,

$$\xi_{max}(t) = \max_{\mathbf{x} \in \partial\Omega_s} \xi(\mathbf{x}, t) \tag{7}$$

where $\partial\Omega_s$ denotes the vessel and aneurysm wall. Associated with this we are also interested in the time-averaged maximal shear stress $\overline{\xi}_{max} = \langle \xi_{max}(t) \rangle$ with $\langle \cdot \rangle$ denoting a time-average over an interval of length T that is long compared to the fluctuation time-scale of the maximum shear stress. This applies for the $Re = 100$ situation. For sufficiently low Reynolds numbers a steady flow develops, for which $\overline{\xi}_{max} = \xi_{max}$. This applies for example at $Re = 10$. An estimate of ξ_{max} is obtained by post-processing individual snapshots of ξ.

The time-dependence of ξ_{max} for the model aneurysm is shown in Fig. 6. We notice a highly fluctuating behavior in ξ_{max} in case of $Re = 100$ that develops around a well-defined average. A constant level in ξ_{max} is observed at $Re = 10$, after a short transient that takes the chosen initial condition to the steady solution. The change in Reynolds number is shown to increase the average shear-stress levels by a factor of about 2. As was discussed

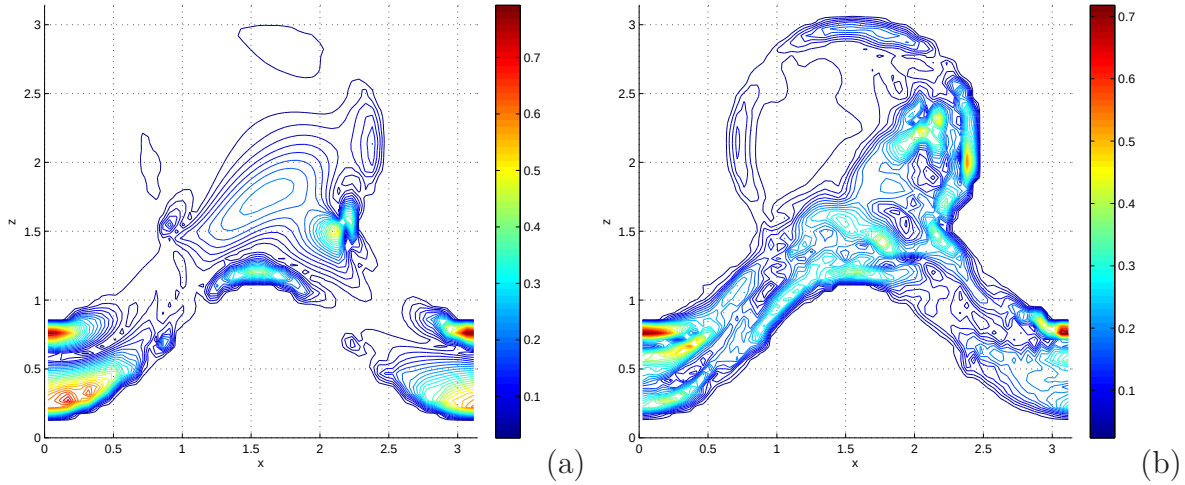

Figure 5: Slices of the normalized shear-stress distribution for the model aneurysm at $Re = 10$ (a) and at $Re = 100$ (b). High shear stress values are distributed near the walls, particularly near the rims of the attached spherical cavity. The spatial resolution is $64 \times 64 \times 64$.

in the previous section, values close to the maximal shear stress arise in the vicinity of sharp edges in the geometry and near comparably rapid changes in the curvature, e.g., near the lower and upper parts of the connecting vessel. Thus, the developing ξ_{max} is directly related to the forces on the wall in the entire domain. We notice that not only the magnitude of the stress but also the level of fluctuations can contribute to the long-time 'wear' of the tissue that makes up the vessel walls.

The precise dependence of $\overline{\xi}_{max}$ on Re is a topic of current investigations. It appears to be correlated with the occurrence of large flow separation when entering the spherical aneurysm cavity. Such topological features of the flow may be a robust indicator of health risk in patients – it is a topic of ongoing research.

5 Concluding remarks

In this paper we presented a basic immersed boundary method (IB) for the prediction of viscous flow in models for cerebral aneurysms. A detailed validation was given, showing a first-order convergence of the numerical solution to Poiseuille flow. We showed in particular that the choice of the masking function is important for the level of accuracy that can be obtained on coarse meshes. It was observed that it is beneficial to define a masking function such that grid cells are part of the 'fluid' domain only if these are entirely embedded within the cylindrical cross-section of the tube.

The flow in curved vessels and in model aneurysms composed of a curved vessel and a comparably large spherical cavity was simulated successfully using the IB approach. Complex flow structures were observed at $Re = 100$, displaying a significant flow separation inside the spherical cavity, while a more smooth flow pattern arises at $Re = 10$. The

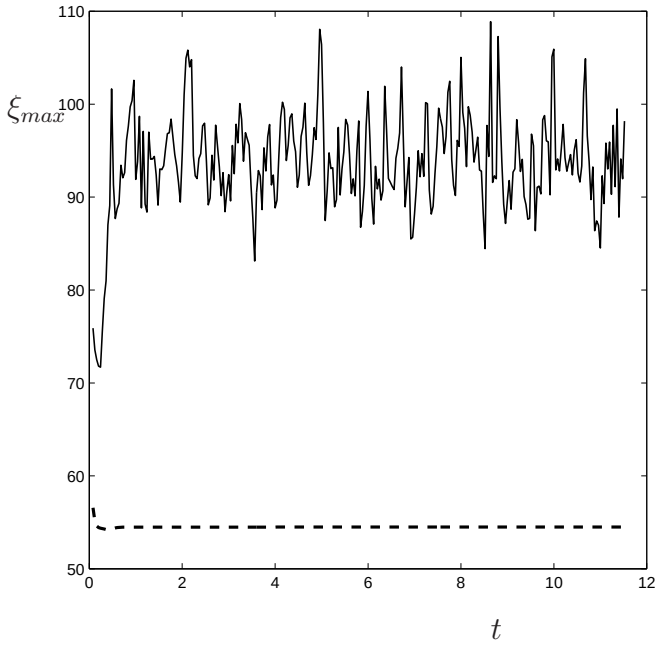

Figure 6: Development of the maximal shear stress ξ_{max} in the model aneurysm, at $Re = 100$ (solid) and $Re = 10$ (dashed).

shear stress on the vessel and aneurysm walls was computed for a steady flow at $Re = 10$ and an unsteady flow at $Re = 100$. The spatial distribution and the general level of shear stress was shown to depend strongly on the Reynolds number. Irregular fluctuations of up to 10% in the maximum shear stress were observed at $Re = 100$. The accuracy with which these shear stresses are obtained will be investigated through a systematic grid-dependence study.

The future application of computational support in the monitoring and treatment of cerebral aneurysms is a field of ongoing research. The location, time-dependence and intensity of the maximal shear stress are all of relevance to medical practice, as these appear to be related to the long-time evolution of the condition of vessel walls. In order to achieve a closer connection with medical practice several steps need to be taken in the computational modeling. A central element is the incorporation of realistic patient aneurysms and their coupling to proper inflow and outflow conditions. As illustrated in this paper, the use of the IB method provides an invaluable point of departure for the geometric representation of complex aneurysms. The inflow and outflow conditions pose a more intricate modeling problem in which the challenge is to approximate patient-specific *in vivo* conditions, e.g., by coupling one-dimensional wave-models to the inflow and outflow planes of actual aneurysms. A second main element is the proper capturing of the interaction between the flow and the structures that make up the aneurysm walls. A model of the mechanical properties of brain tissue near aneurysms needs to be incorporated that allows a patient-specific inclusion of 'material parameters'. In all these aspects, attention

should be given to the computational robustness of predictions, focusing on the relation between the general topology of flow structures and the shear stress characteristics.

Acknowledgments

The authors would like to thank Dr. W.-P. Breugem of Delft University of Technology for stimulating discussions on the relation between the definition of the masking function and general error-levels in the numerical solution.

REFERENCES

[1] R. Mittal and G. Iaccarino, Immersed Boundary Methods, *Annu. Rev. Fluid Mech.*, **37**, 239–261 (2005).

[2] G. G. Ferguson, Turbulence in Human Intracranial Saccular Aneurysms, *J. Neurosurg.*, **33**, 485–497 (1970).

[3] M. E. Sprengers, J. Schaafsma, W. J. van Rooij, M. Sluzewski, G. J. E. Rinkel, B. K. Velthuis, J. C. van Rijn and C. B. Majoie, Stability of Intracranial Aneurysms Adequately Occluded 6 Months after Coiling: A 3T MR Angiography Multicenter Long-Term Follow-Up Study, *American Journal of Neuroradiology*, **29**, 1768–1774 (2008).

[4] M. Grass, R. Koppe, E. Klotz, R. Proksa, M. H. Kuhn, H. Aerts, J. Op de Beek and R. Kemkers, Three-dimensional reconstruction of high contrast objects using C-arm image intensifier projection data, *Computerized Medical Imaging and Graphics*, **23**, 311–321 (1999)

[5] J. Hendrikse, A. F. van Raamt, Y. van der Graaf, W. P. T. M. Mali and J. van der Grond, Distribution of Cerebral Blood Flow in the Circle of Willis, *Radiology*, **235**, 184–189 (2005)

[6] R. W. C. P. Verstappen and A. E. P. Veldman, Symmetry-Preserving Discretization of Turbulent Flow, *J. Comput. Phys.*, **187**, 343–368 (2003).

[7] G. K. Batchelor, An Introduction to Fluid Dynamics, *Cambridge University Press*, (2000).

[8] B. J. Geurts, Elements of Direct and Large-Eddy Simulation, *Edwards Publishing*, 2003.

[9] J. Mikhal, D. J. Lopez Penha, S. Stolz, and B. J. Geurts, Application of an Immersed Boundary Method to Flow in Cerebral Aneurysms and Porous Media, To appear: In proceedings of the *Fluids Engineering Summer Meeting*, ASME 2010, Montreal, Canada (2010)